Chapter 2 Physical Fundamentals of Chemical Vapour Deposition

The CVD techniques rely on the gases which are transported into a reaction chamber for deposition. In this chapter, the fundamental physics relating to these techniques are introduced to enable a thorough theoretical understanding of the phenomena occurring in a CVD process and the process control parameters. The topics introduced in this chapter include basic gas laws and kinetic theory, vacuum technology, gas transport phenomena and vapour pressures of some commonly used CVD reactant gases.

2.1 Gas Laws and Kinetic Theory

To study gas movement, some basic assumptions are commonly made to facilitate the understanding of the flow behaviour of the gases for a CVD process. Based on these assumptions the investigation can then focus on theory and practice of what is termed an ideal or perfect gas. This is a theoretical concept which corresponds to and is based upon the following assumptions:

1. the molecules themselves are very small spheres and a gas consists of a huge number of particles;
2. the volume of all molecular spheres is much smaller than that actually occupied by the gas;
3. the molecules are independent such that they do not exert any force on each other;
4. they move randomly along rectilinear paths;
5. the molecules are considered to be rigid solids and they make perfect elastic collisions.

Some real gases, such as elements in the periodical table of elements (e.g. H_2, N_2, O_2 and Ar) and gases used in a CVD process (e.g. CH_4 and CH_3SiCl_3 etc.), exhibit the approximate behaviour of ideal gases at atmospheric pressures. At lower pressures (vacuum) many more gases can be treated as the ideal gases. Based on the above assumptions and the model of kinetic theory of gases, the following specific laws of the gases have been generalized and established [1, 2].

2.1.1 Gas Laws

2.1.1.1 Boyle's Law
Ideal or perfect gases obey Boyle's law at all temperatures. This fact was established by Boyle and Mariotte in 1662. According to this law, the product of P and V is constant for a given mass of gas at a constant temperature, where P is the pressure of the gas and V is its volume.

$$PV = \text{const} \tag{2.1}$$

2.1.1.2 State Equation of an Ideal Gas

The volume of a gas is directly proportional to the absolute temperature and inversely proportional to the pressure. This is expressed as

$$PV = nRT \tag{2.2}$$

where n is the number of gas molecules in a mole and R is the universal gas constant ($8.31 \text{J} \cdot \text{K}^{-1} \cdot \text{mol}^{-1}$)

2.1.1.3 Dalton's Law of Partial Pressures

The total pressure exerted by a mixture of gases is equal to the sum of the partial pressures exerted by the individual components. This empirical law was observed by John Dalton in 1801 and is expressed by

$$P_{tot} = p_1 + p_2 + p_3 + ... + etc. \tag{2.3}$$

where P_{tot} is the total pressure and p_1, p_2, p_3 and so on are the pressures of an individual gas in a gas mixture.

2.1.1.4 Partial Pressures

The partial pressure exerted by any one component of a mixture of gases is the pressure exerted by the component gas as if it occupied that whole volume alone.

2.1.1.5 Avogadro's Law

Equal volumes of all ideal gases measured at the same temperature and pressure contain the same number of molecules. This law was hypothesised by Amedeo Avogadro in 1811.

2.1.1.6 Avogadro's Number

The number of molecules in one mole of a gas or any gas substance is a universal constant value of 6.02×10^{23}.

2.1.1.7 Mole Volume

The volume occupied by a mole molecule of a gas is a universal constant found experimentally to be 22.4 litres under standard conditions, i.e. a pressure of 101.3 kPa and a temperature of 273 K.

In accordance with the perfect gas laws, the densities of some gases used in CVD processes are listed in Table 2.1. It is clear that there exist considerable density differences for various gases. For the CH_3SiCl_3–H_2 reaction system, the density of the CH_3SiCl_3 gas is 75 times greater than that of H_2 under standard conditions. To obtain a homogeneous mixture of the gases, it is necessary to mix the individual gases homogeneously before they are introduced into the reaction chamber. In addition, N_2 or Ar is usually employed as a purge gas before and after

Table 2.1. Density of some gases for CVD applications (at 25°C, 1 atm)

Species	M (g·mol⁻¹)	ρ (g·l⁻¹)	Species	M (g·mol⁻¹)	ρ (g·l⁻¹)	Species	M (g·mol⁻¹)	ρ (g·l⁻¹)
Ar	40	1.79	CH_4	16	0.71	$SiCl_4$	170	7.59
H_2	2	0.09	C_3H_6	42	1.875	$TiCl_4$	190	8.48
N_2	28	1.25	NH_3	17	0.76	$ZrCl_4$	233	10.40
O_2	32	1.43	SiH_4	32	1.43	WF_6	298	13.30
Air	29	1.29	$AlCl_3$	133.5	5.96	CH_3SiCl_3	149.5	6.67
CO_2	44	1.96	BCl_3	117.5	5.25	$Mo(CO)_6$	264	11.79
H_2O	18	0.80	$ReCl_5$	363.5	16.23	$Ir(acac)_3$	489	21.83

Note: $Ir(acac)_3$ stands for $Ir(C_5H_7O_2)_3$

the CVD process. The reason is that the density of N_2 gas is almost the same as that of air, and the density of Ar gas is slightly greater than that of air. Therefore, such a purge gas is very helpful in avoiding the contamination of the water vapour from the air in the chamber.

2.1.2   Gas Kinetic Theory

Gas kinetic theory, for the purposes of this book, consists of the relationships defining the simple pressure, gas velocity distribution, mean free path and impinging flux of gases to the surface of a substrate, and other relevant theoretical relationships. These collective descriptions of the gases form a set of comprehensive theoretical understanding and representation for CVD processes. The following subsections briefly describe this constituent theory.

2.1.2.1 Pressure
Pressure is defined as the force per unit area which a gas exerts on the surface and is given by

$$P = \frac{1}{3} Nmu_{av}^2 \tag{2.4}$$

where P is the pressure, N is the molecular number per unit volume, m is the mass of molecule and u_{av} is the mean velocity of the gas molecules. There are many kinds of units for the pressure of a gas; the conversion factors are listed in Appendix A.

2.1.2.2 Maxwell–Boltzmann Distribution

Molecules travel at different velocities. The Maxwell–Boltzmann distribution of velocity is used to define the velocity profile of molecules and is written as

$$f(u) = 4\pi(\frac{m}{2\pi kT})^{3/2} u^2 \exp(-\frac{mu^2}{2kT}) \tag{2.5}$$

where $f(u)$ is the probability of a molecule having a certain velocity, m is the mass of one molecule, k is the Boltzmann constant $(1.38 \times 10^{-23}$ J·K$^{-1})$, u is the magnitude of the velocity of a molecule and T is the temperature in Kelvin.

The most probable velocity, u_p, is the velocity most likely to be possessed by any molecule in the system and corresponds to the maximum value or mode of $f(u)$:

$$u_p = \sqrt{\frac{2kT}{m}} = \sqrt{\frac{2RT}{M}} \tag{2.6}$$

where M is the mole mass of the gas.

The mean velocity is the mathematical average of the velocity (u_{av}) distribution:

$$u_{av} = \int_0^\infty uf(u)du = \sqrt{\frac{8kT}{\pi m}} = \sqrt{\frac{8RT}{\pi M}} \tag{2.7}$$

For nitrogen at 298 K, substituting $k = 1.38 \times 10^{-23}$ J·K^{-1}, and $M = 28$ g·mol^{-1}. Then, the average velocity is 475 m·s^{-1}, which is much faster than that of the speed of sound. This implies that the thermal movement of gaseous molecules is very intense.

The root mean square velocity, u_{rms}, is the square root of the average squared velocity.

$$u_{rms} = \sqrt{\int_0^\infty u^2 f(u)d(u)} = \sqrt{\frac{3kT}{m}} = \sqrt{\frac{3RT}{M}} \tag{2.8}$$

Figure 2.1 shows the velocity distribution of hydrogen gas at different temperatures ranging from 298 K to 1273 K. The most probable velocity, the mean velocity and the root mean velocity increase with increases in temperature. Moreover, there are more molecules with a higher velocity at higher temperatures because the curve becomes flatter.

The above three velocities have been defined to measure the velocity of molecules from different viewpoints. Three kinds of velocities are used for different applications: the root mean square velocity (u_{rms}) is used for the calculation of the average dynamic energy, the mean velocity u_{av} for the mean distance between molecules, and the most probable velocity (u_p) for the distribution of velocity.
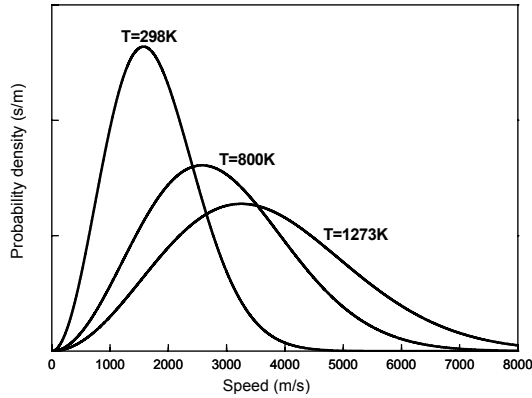
Figure 2.1. Velocity distribution of H_2 gas at different temperatures

These velocities are inherently used to express the same molecular behaviour, and therefore there is a close relationship among them, which is defined as follows:

$$u_{av} = 1.128u_{p,}\ u_{rms} = 1.225u_p \tag{2.9}$$

2.1.2.3 Mean Free Path

Though molecules travel at a very high speed, over 400 m per second at ambient temperature, they do not travel in straight lines. They frequently collide with other molecules as they travel. Hence they bounce around and form a zigzag pattern as shown in Figure 2.2.

The molecules in a gas are in constant random motion, periodically colliding with one another and moving off in new directions. The average distance that a molecule moves before colliding with another molecule is called the mean free path and is given by
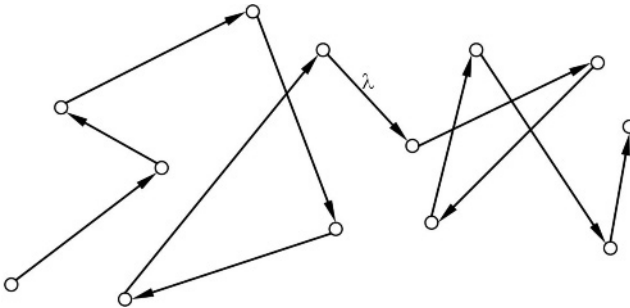
$$\lambda = \frac{kT}{\sqrt{2}\pi P d^2} \tag{2.10}$$

Figure 2.2. Schematic of gas molecule movement and mean free path

where d is the molecular diameter, T is the temperature in *Kelvin*, k is the Boltzmann constant and P is the pressure.

At room temperature, a simple expression is used for the calculation of the mean free path of air [3]:

$$\lambda = \frac{5\times10^{-3}}{P}\ (\text{cm}) \tag{2.11}$$

where P is the pressure in torr.

According to Equation 2.10, λ differs for various gases and is inversely proportional to the pressure. Table 2.2 lists the diameters, mean free path and three commonly used velocities of some typical gases.

Table 2.2. Molecular diameters, mean free path and velocities of some gases

Gas	M (g/mol)	$d\ (\times10^{-10}\ \text{m})$	$\lambda(\times10^{-8}\ \text{m})$	u_p (m/s)	u_{av} (m/s)	u_{rm} (m/s)
Air	29	3.76	6.48	413	466	506
Ar	40	3.69	6.73	352	397	431
B_2H_6	28	4.70	4.15	421	475	515
$Ba(thd)_2$	503	9.38	1.04	99	112	122
CH_4	16	4.18	5.25	557	628	681
C_2H_2	26	4.96	3.73	436	492	534
CH_3SiCl_3	149.5	5.11	3.51	182	205	223
Cl_2	71	5.51	3.02	264	298	324
CO_2	44	4.66	4.22	335	379	411
$Cu(thd)_2$	429.5	9.34	1.05	107	121	132
H_2	2	2.83	11.44	1574	1776	1927
He	4	2.20	14.09	1113	1256	1363
N_2	28	3.78	6.41	421	475	515
NH_3	17	4.57	4.39	540	609	661
O_2	32	3.61	7.03	393	444	483
SiH_4	32	4.08	5.51	393	444	483
$Si(OC_2H_5)_4$	208	6.90	1.92	154	174	189
WF_5	279	5.21	3.38	133	150	163
WF_6	298	5.21	3.38	129	145	158
$Y(thd)_3$	638	10.7	0.8	88	99	108

Note: 1. Gases are at the conditions of 25°C, 1 atm,
        2. thd: 2,2,6,6-tetramethyl-3,5-heptandionate, $C_{11}H_{19}O_2$

It should be noted that the mean free path is different from the average distance between molecules. Considering the example of N_2 gas at 25°C and 1 atm, the mean free path and mean distance are 6.42×10^{-8}m and 3.34×10^{-9}m, respectively. It is clear that the mean free path is one order greater than the mean distance. Due to molecules with small size but high velocity of thermal movement, gaseous molecules are unlikely to collide with each other quickly, hence resulting in a larger mean free path.

2.1.2.4 Knudsen Law (Cosine Law) [4]

In an equilibrium state, the number of the gaseous molecules impinging onto a specific area obeys the Cosine law, or Knudsen law. The details are explained as follows.

It is assumed that the gaseous molecules are equally distributed in all directions at all the places and they move randomly. For a specific area (dA) on the inner surface of a chamber, the probability of the molecules moving from the solid angle ($d\omega$) is equal to $d\omega/4\pi$. It is noted that there is an inclusion angle (θ) formed between the normal line of this area and the solid angle, as shown in Figure 2.3. For the molecules within the velocity range from u to $u+du$, the number of the molecules (dN) impinging onto the dA area in the unit time from the solid angle is given by

$$dN = \frac{d\omega}{4\pi} n \cdot f(u) \cdot u \cdot \cos\theta \cdot dA \qquad (2.12)$$

where n is the number of molecules within the unit volume and $f(u)$ is the Maxwell–Boltzmann distribution function in Equation 2.5.

By integrating the velocity from 0 to infinity, the total number of molecules impinging on the area of dA is given by
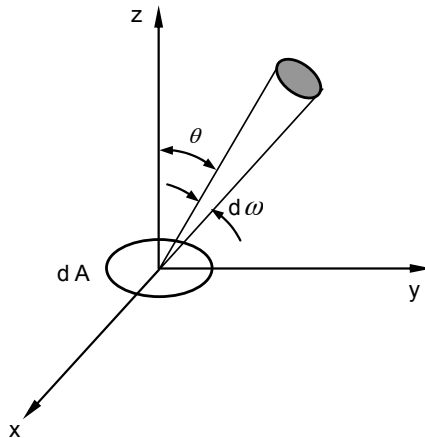

Figure 2.3. Schematic of Knudsen's law

$$N = \frac{d\omega}{4\pi} n \cos\theta dA \int_0^\infty u f(u) du = \frac{d\omega}{4\pi} n u_{av} \cos\theta dA \qquad (2.13)$$

The cosine law of Equation 2.10 means that the number of molecules impinging on an area is proportional to the cosine function of the angle (θ).

To explain the significance of this law, Knudsen assumed that a molecule is wholly adsorbed by the surface of a solid and remains on the surface for a period of time; it is subsequently "rebounded" from the surface in a direction which does not depend on the incidence angle or its history before the adsorption takes place. This explanation has been confirmed and validated by considerable experimental observations.

The residence time (τ) of a molecule on the surface is of interest in understanding a CVD mechanism, and the following expression has been established [5]:

$$\tau = \tau_0 \exp(-\frac{Q}{RT}) \qquad (2.14)$$

where τ_0 is equal to the period of the gas molecule vibration, which should be of the order of 10^{-13} s, and Q is the adsorption heat. For example, for CO on the crystal plane (111) of Pd, the residence time over the temperature range of 580 to 700 K is in the range of 0.1 to 10 ms.

According to the cosine law, the number of gas molecule collisions on a wall in per unit area and per unit time is given by

$$n_0 = \frac{1}{4} n u_{av} \qquad (2.15)$$

where n is the number of gas molecules in unit volume.

2.1.2.5 Hertz–Knudsen Law

During the CVD process, the molecules to be incorporated into the lattice of substrate must be delivered to the surface from the bulk gas. The flux of incident molecules onto the substrate surface is defined by the Hertz–Knudsen equation [3, 6]:

$$F = \frac{P}{\sqrt{2\pi MRT}} \ [\text{mole·cm}^{-2}\text{·s}^{-1}] \qquad (2.16)$$

where P is the gas pressure in torr, M is the mole mass of the gas in g·mol^{-1} and T is the absolute temperature in Kelvin.

Another useful expression is given by [3, 6]

$$F = 3.35 \times 10^{22} \frac{P}{\sqrt{MT}} \ [\text{molecules·cm}^{-2}\text{·s}^{-1}] \qquad (2.17)$$

2.2 Vacuum Technology

A vacuum vessel or chamber is normally required to create a suitable environment for a CVD process to take place. The quality and the controllability of such a vacuum environment are critical to a CVD process. The technologies associated with vacuum generation and maintenance is therefore important and is described in this section.

2.2.1 Definition and Classification of Vacuum

The constituents of the normal atmosphere are mainly nitrogen and oxygen in the ratio of 80% to 20%, together with a small amount of rare gases, such as carbon dioxide, argon, neon and helium and a variable quantity of water vapour depending on ambient temperature and humidity conditions. The abundance of each gas can be conveniently expresses as either mass percentage, volume percentage or the pressure that each constituent gas contributes to the total. The detailed values of these measurements for each gas are listed in Table 2.3.

Table 2.3. Composition of dry atmospheric air at sea level [7]

Component	Mass(%)	Volume(%)	Partial pressure(kPa)
N_2	75.51	78.1	79.2
O_2	23.01	20.93	21.2
Ar	1.29	0.93	0.947
CO_2	0.04	0.83	3.1×10^{-2}
Ne	1.2×10^{-3}	1.8×10^{-3}	1.9×10^{-3}
He	7×10^{-5}	7×10^{-5}	5.3×10^{-4}
CH_4	2×10^{-4}	2×10^{-3}	2×10^{-4}
Kr	3×10^{-4}	1.1×10^{-4}	1.1×10^{-4}
N_2O	6×10^{-5}	5×10^{-5}	5×10^{-5}
H_2	5×10^{-6}	5×10^{-5}	5×10^{-5}
Xe	4×10^{-5}	8.7×10^{-6}	9×10^{-6}
O_3	9×10^{-6}	7×10^{-6}	7×10^{-6}
	$\Sigma100\%$	$\Sigma100\%$	$\Sigma101.3$
50%RH at 20°C	1.6	1.15	11.7

Note: water vapour pressure is 7 Torr and varies largely according to the humidity

According to the definition of the American Vacuum Society originally defined in 1958, the vacuum is defined as the fact that a given space filled with gas at pressure below the atmospheric pressure, i.e. having a density of less than about

2.5×10^{19} molecules·cm^{-3}. The general term of vacuum includes nowadays about 19 orders of magnitude of pressures (or densities) below that corresponding to the standard atmosphere. Considering the atmospheric pressure to be 10^5 Pa, the vacuum definition using the above standard is at a pressure of 10^{-14} Pa [3].

A perfect or absolute vacuum implies the unrealisable state of space entirely devoid of matter, which is extremely difficult to achieve. For practical purposes, four levels of vacuum are defined for CVD processes. To be more specific, these four pressure ranges and some features are listed in Table 2.4.

A CVD process is generally performed in a vacuum condition. The two main factors that require a vacuum condition are (1) to remove or minimise the active atmospheric constituents that could cause undesirable physical or chemical reactions (especially oxygen and water vapour) and (2) to improve the coating uniformity by increasing the mean free path of precursor gases. As the pressure is decreased from its atmospheric value of almost 760 Torr to 0.5 to 1 Torr, the free mean path increases by a factor of 1000, as shown by Equation (2.10).

Most CVD systems operate in the low or medium vacuum regimes. To ensure a clean chamber, however, CVD systems are often pumped into the high vacuum regime before introducing the reactant precursor gases.

In order to express the state of a vacuum system, various sources of undesirable gases existing in the system must be considered to reflect the dynamic equilibrium during the pumping process. The sources of gases in a vacuum system are as follows:

1. the gas molecules of the initial atmosphere enclosed in the vacuum system;
2. the gas which penetrates into the system as a result of leakage, especially from the areas where there are moving parts and sealing elements, causing

Table 2.4. Classification of vacuum

	Low vacuum	Medium vacuum	High vacuum	Ultra high vacuum
Pressure (Torr)	760–1	1–1×10^{-3}	10^{-3}–10^{-8}	$<10^{-8}$
Pressure (Pa)	1.01×10^5 -1×10^2	10^2–10^{-1}	10^{-1}–10^{-6}	$<10^{-7}$
Number of molecules in cm^3	2.69×10^{19} -3.54×10^{16}	3.54×10^{16} -3.54×10^{13}	3.54×10^{13} -3.54×10^{8}	$<3.54\times10^{8}$
Mean free path (cm)	6.7×10^{-6} -5.1×10^{-3}	5.1×10^{-3} -5.1	5.1 -5.1×10^{-5}	$<5.1\times10^{-5}$
Molecule incidence rate (molec·cm-2·s-1)	2.87×10^{23} -3.78×10^{20}	3.78×10^{20} -3.78×10^{17}	3.78×10^{17} -3.78×10^{12}	3.78×10^{12}
Flow characteristics	Continuum flow	Transition region	Free molecular flow	Molecule motion

wear and further leakage;
3. the gas desorbed from the thermal insulator materials with the porous structure and the cold surface of the chamber;
4. the gas entering the system by permeation through walls and windows; and
5. the gas delivered into the reaction chamber for the CVD process.

Taking into consideration the above factors, it is possible to understand the influence of various gas sources on the vacuum system and how to design such a vacuum system. It is helpful to use this understanding to judge if the vacuum system is in good condition, as well as to analyse and eliminate any problems with the vacuum that might arise.

2.2.2   Quantitative Description of the Pumping Process

The conductance C of a duct (or a pipe) for a flow of gas is the rate of flow under pressure gradient. As shown in Figure 2.4, it is used to measure the ease of gas flow and defined by [7, 8]

$$C = \frac{Q}{P_1 - P_2} \tag{2.18}$$

where P_1 and P_2 are the pressure at the inlet and at the outlet of a duct, respectively, Q is the flow throughput.
    If the duct is assumed smooth, round, straight and sufficiently long (L >> d), the conductance for the viscous flows can be expressed as

$$C_v = \frac{\pi d^4 P}{128 \mu L} \tag{2.19}$$

For molecular gas flows, the conductance is given by

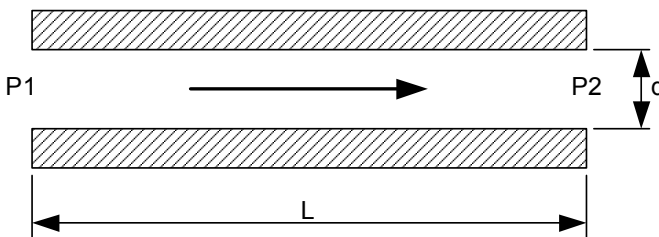$$C_m = \frac{1}{6} \sqrt{\frac{2 \pi R T}{M}} \cdot \frac{d^3}{L} \tag{2.20}$$

Figure 2.4. Conductance of gas flow in a pipe

For intermediate flows, the expression is given as

$$C_t = C_v + \frac{1 + c_1 P}{1 + c_2 P} C_m \tag{2.21}$$

where c_1 and c_2 are two constants related to the gas species and pipe diameter, M is the molar mass of the gas, P is the average pressure along the pipe, R is the gas constant and T is temperature.

For the air at a temperature of 20°C, its viscosity is 18.2×10^{-6} Pa·s, and the above conductance expressions can be rewritten as follows:

$$C_v = 1.366 \frac{d^4 P}{L} \tag{2.22}$$

$$C_m = 12.1 \frac{d^3}{L} \tag{2.23}$$

$$C_t = \frac{d^3}{L} [136.5 dP + 12.1(\frac{1 + 192 dP}{1 + 237 dP})] \tag{2.24}$$

It is important to note that in the molecular flow regime the conductance depends on the cube of the diameter of the tube and the $-1/2$ power of the mole mass of the gas being pumped, but the conductance is independent of the pressure.

For the parallel connection of the ducts, the total conductance (C) is the sum of all individual conductances and is given by [9]

$$C = C_1 + C_2 + \cdots + C_n \tag{2.25}$$

where C_1, C_2 and C_n are the different individual conductances respectively.

For the series connection of the ducts, the total conductance (C) is expressed by [9]

$$\frac{1}{C} = \frac{1}{C_1} + \frac{1}{C_2} + \cdots + \frac{1}{C_n} \tag{2.26}$$

Because of the resistance to gas flow in the connection between a vacuum chamber and the pump, the effective pump volume speed (S) at the chamber is usually less than the volume flow rate of the pump (S_p) at its inlets. The relationship between S and S_p is given by [3]

$$\frac{1}{S} = \frac{1}{C} + \frac{1}{S_p} \tag{2.27}$$

where C is the effective conductance of the system from the pump to the vacuum chamber and S_p is the pumping speed.
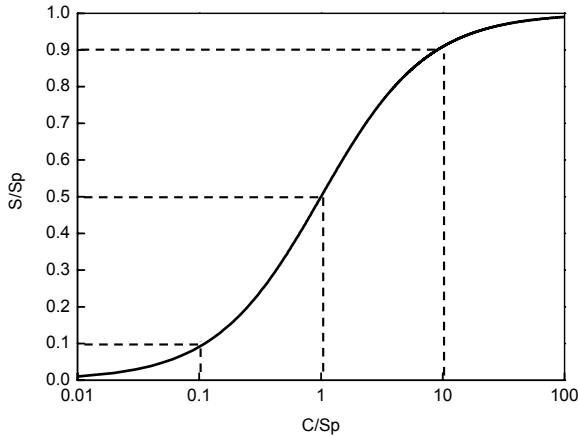
Figure 2.5. Relationship between S/S$_p$ and C/S$_p$

In Figure 2.5, it can be seen that S/S_p only reaches 50% if the value of the conductance equals that of the pumping speed, i.e. the ratio of C/S_p equals 1. $S/S_p =$ 90% can be achieved when the conductance is 10 times S_p. If the conductance is much less than S_p, then S is determined entirely by the conductance of the duct but not by the speed of the pump. For this reason, it is not useful to increase the pump performance or speed if the conductance of the pipe is the limiting factor. To ensure sufficient conductance, it is necessary to minimise the duct length between the vacuum chamber and the vacuum pump, as well as to use the duct with a large enough diameter.

2.2.3 Vacuum Pumps

2.2.3.1 Vacuum Pump Parameters and Classification

The pump parameters are used to define the behaviour of a pump system and are very important in selecting a suitable pump and in designing a vacuum system. These parameters mainly include the lowest pressure, pressure range, pumping velocity and exhaust pressure. The selectivity of the pump and the compositions of the residual gases are the additional parameters if the ultra-high vacuum is required in some applications. The following sections give more detailed definitions and descriptions of these parameters [3].

Lowest Pressure

The lowest pressure is the extreme low pressure which can be achieved by a vacuum pump at its inlet. This pressure is mainly dependent on the working principle of a vacuum system and the type of pumps used in such a system. For a given vacuum pump, the lowest pressure is determined either by the leakage pressure in the pump itself, at which point the pump becomes ineffective in maintaining the desirable pressure, or by the vapour pressure of the fluid used.

Pressure Range

The pressure range is the pressure difference of the maximum pressure and the minimum pressure in which a vacuum pump can work efficiently. It is necessary to combine the different types of pumps together to generate high vacuum pressure.

Pumping Speed

Pumping speed is defined as the volume of gas evacuated by a pump within the unit time. It is expressed by

$$S_P = \frac{dV_{P,T}}{dt} \tag{2.28}$$

where S_P is pumping speed, t is time, $V_{P,T}$ is the gas volume evacuated under a pressure P and at a temperature T. It is an important parameter for selecting the capacity of a pump according to the size of the vacuum chamber for a given CVD process.

Exhaust Pressure

The exhaust pressure is the pressure at the outlet of a pump. If the maximum pressure of a pump is lower than the atmospheric pressure (e.g. roots pump and oil diffusion pump), it must be backed with a mechanical rotary pump. In addition, some types of pumps have no outlet, such as ionisation and sorption pumps.

Vacuum pumps are generally divided into 13 categories according to the working principle, as listed in Table 2.5. They include water jet pump, water ring pump, steam ejector, oil-sealed rotary pump, Roots pump, vacuum diffusion pump, oil vapour booster pump, sputtering-ion pump, radial field pump, titanium sublimation pump, sorption pump, molecular pump and cryopump [9].

Table 2.5. Vacuum pump classification and related parameters

Vacuum pump	Maximum capacities (l·s^{-1})	Operating pressure range (Torr)
Water jet pump	500	760 to 15~25
Water ring pump	1 to 2500	760 to 100 (1 stage), 760 to 25 (2 stage)
Steam ejector	100,000	760 to 75 (1 stage), 125 to 20 (2 stage)
		30 to 2.5 (3 stage), 5 to 0.03 (4 stage)
Oil-sealed rotary pump	0.25 to 500	760 to 2×10^{-2}(1 stage), 760 to 5×10^{-3} (2 stage)
Roots pump	50 to 35,000	10 to 10^{-3}
Vacuum diffusion pump	95,000	From 10^{-2} to 10^{-9}
Oil vapour booster pump	23,000	1 to 10^{-4}

Table 2.5. (continued)

Sputtering-ion pump	7,000	10^{-2} to below 10^{-11}
Radial field pump	400 to 800	10^{-4} to below 10^{-11}
Titanium sublimation pump	Thousands	10^{-3} to below 10^{-11}
Sorption pump	1,000	760 to 10^{-2} (1 stage), 760 to 10^{-5} (multistage)
Molecular pump	10,000	10^{-1} to 10^{-10}
Cryopump	Million	10^{-3} to below 10^{-10}

Because of the large gas output involved in some CVD processes, a combination of a rotary pumping system with a Roots pump is commonly used to give the desired output flow rate. Since the rotary pump works in an oil environment, the current trend is to replace the rotary pumps with dry pumps, which operate without oil, to reduce oil contamination. For very low pressure operation, a turbomolecular pump is used to provide an extra-high vacuum. For the halides, the Roots pump is still used since turbomolecular pumps do not withstand long operation in acid conditions. An additional turbomolecular or cryogenic pump-based system is commonly used to ensure reactor cleanliness before actual runs of the gases in the reaction chamber, with the typical pressure in the 10^{-9} Torr range.

The following section describes the working principles of the mechanical rotatory pump and the Roots pump, as well as related topics.

2.2.3.2   Mechanical Pumps

Principle and Characteristics

Mechanical pumps are used directly to produce a low and medium vacuum, as well as extensively to back Roots vacuum, turbomolecular and diffusion pumps. These pumps are also called oil-sealed rotary vane pumps as they rely on the use of vanes or blades to compress gases.

A rotary vacuum pump is essentially a gas compressor. The mechanism of the pump is designed such that it has an eccentric blade or vane rotating to cause four distinctive actions, namely gas introduction, isolation, compression and gas exhaust. The working principle of the mechanism is therefore divided into four steps during the rotation of the vanes, as illustrated in Figure 2.6:

1. Gas is introduced into the pump from a working chamber to be vacuumed.
2. Then the gas is isolated into the pump cavity between the rotor and the stator by the vanes when they rotate passing the seal-off point.
3. The trapped gas is continuously compressed by the rotation of the rotary vane. As the rotor is eccentric to the inner surface of the stator, the further rotation of the vanes compresses the gas into a smaller space. During this operation, the vanes loaded by the spring and helped by the centrifugal force can seal the contact area even though they are rotating eccentrically.
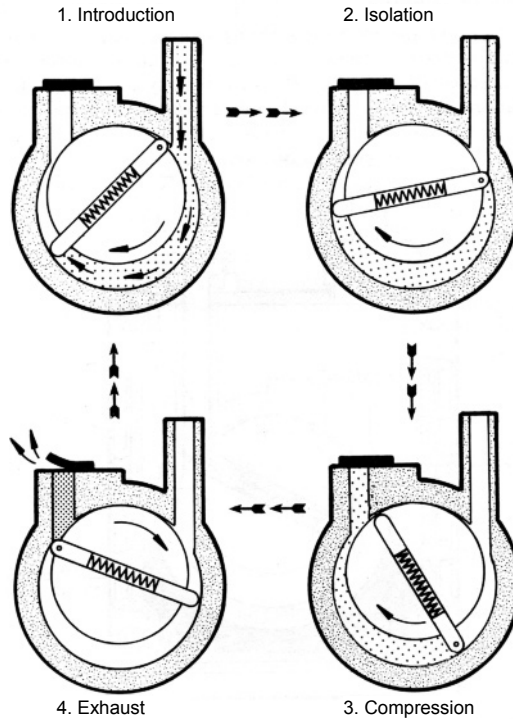
Figure 2.6. Working principle of a rotary van pump [10]

4. The compressed gas is either flushed out to the atmosphere via the controlled exhaust valves or conveyed to the next stage for further compression.

These pumps are immersed in the oil during operation. Oils are used on the one hand to lubricate the moving parts, e.g. rotor, vanes and contact between rotor and stator, and on the other hand, to seal the rubbing interface between the stator and the vanes. Gas leakage between the rotor and stator interfaces is prevented by a close contact between the vanes and the stator. The centrifugal force also helps the vanes to keep in close contact with the stator. The seal between the stator and vane blades is created by a thin layer of oil film formed by the small quantity of oil between the stator and rotor surface. A vane rotor pump with a good oil sealing can achieve a compression ratio (the ratio of pressure at the outlet to that at the inlet) of as high as 10^5 or 10^6.

In theory, the lowest pressure achieved by oil-sealed rotary vane pumps is determined by the outlet pressure which can be discharged either to the atmosphere or the inlet of the next stage of the vane pumps. When the exhaust gas pressure becomes lower than the atmospheric pressure, the gas trapped inside the pump cannot be discharged. If the inlet pressure of 10^{-2} Torr is produced for the
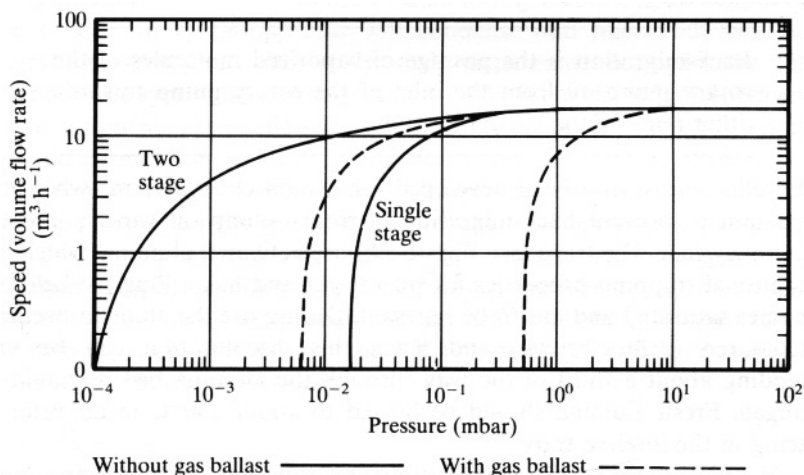
Figure 2.7. Pumping velocity versus pressure curves of mechanical pump [10]

atmospheric exhaust pressure, then the compression ratio of the pump should reach the order of 10^5. If an even lower inlet pressure is desired, it is necessary to introduce the next stage of pumping action.

In cases of such requirements, the lowest pressure can be further reduced by using two stages of a pump configured in series. The first stage, usually called the high vacuum stage, is connected to the second stage, called the low vacuum stage, through an internal duct. This series arrangement enables the exhaust pressure of the high vacuum stage to discharge the gas at a pressure much lower than atmospheric pressure, due to a second compression at the low vacuum stage. The lowest pressure of a single-stage rotary pump is usually 5×10^{-2} Torr, and the two-stage pumps can achieve a 1×10^{-4} Torr inlet pressure, thereby giving two-stage pumps a higher compression ratio close to 10^7.

The speed curve of a mechanical rotary pump is shown in Figure 2.7. The pumping speed is nearly a constant in the pressure range of 760 to 10 Torr. Then, it is significantly decreased when the pressure is below 10 Torr. Furthermore, the speed decrease of a single-stage pump is much more rapid than that of a two-stage pump. The pumping speed becomes zero when the pressure reaches the lowest value.

The performance of the mechanical pump is mainly dependent on the finish of the parts, the sealing between the tips of the vanes of the rotator and the bore of the stator and between the sides of the vanes and the rotator. The suitable spacing between the vanes and the slot of the rotator is typically in the range of 0.04 to 0.1 mm. If the gap is too small, the vanes may be "stuck" within the slot, thereby decreasing the rotation speed and the pumping efficiency. If the gap is too large, leakage occurs, resulting in lower vacuum generated.

Gas Ballast

For mechanical pumps, the potential condensation of vapours from the work chamber can cause problems for the pumps, especially for a CVD process. The compression of the vapour leads to condensation, which forms liquid droplets, if the partial pressure of a gaseous vapour reaches its saturated vapour pressure of a liquid. These condensed liquid droplets may contain water, HCl and some chlorosilanes. They mix with the pump oil and result in corrosion of pump parts. For example, the vapour pressure of methyltrichlorosilane (a kind of precursor for SiC deposition) at 28°C is about 200 Torr. If this gas is compressed by a factor of 10^7 by a two-stage pump, methyltrichlorosilane will be condensed if its partial pressure in the reaction chamber is more than 2×10^{-5} Torr.

In order to solve this problem, a gas ballast valve was first designed by Gaede in 1935 [3], as shown in Figure 2.8, which periodically injects a small amount of air, or an inert gas such as N_2 [11], into the pump in a controlled manner at the
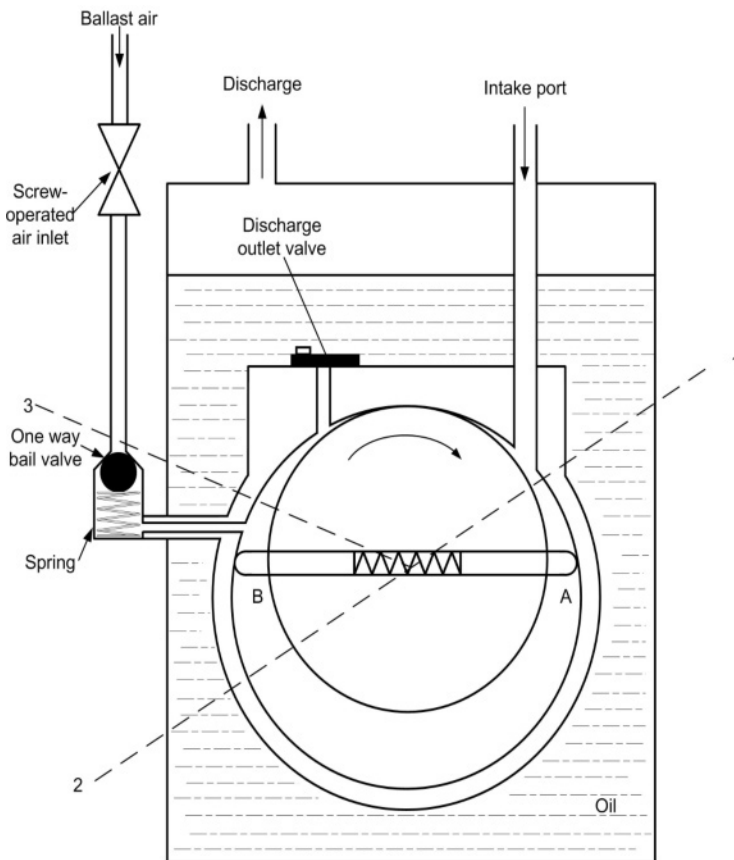
1, 2 and 3 denote successive positions of A during a revolution

Figure 2.8. Working principle of the gas-ballast pump [12]

compression stage. The leading vane, A, rotates from position 2 to position 3, and the valve is open, resulting in the introduction of air into the pump. During this period, the isolated gas is not compressed. Instead, the injected air mixes with the isolated gas. When the mixture of the gases reaches the ejection pressure at the outlet port, the partial pressure of the vapour remains below its saturated pressure such that it can prevent the condensation of the vapour, as shown by the dashed line in Figure 2.7. In such a case, the lowest pressure of the pump is dropped by two orders of magnitude.

Pump Oil

Pump oil plays an important role in oil-sealed mechanical pumps. Its primary functions in such a system include [7, 12]

- lubrication of mechanical moving parts such as the bearings of the rotor, the spring-loading sliding vanes onto the rotor, and rubbing surfaces between the tips of the vanes and the inner surfaces of the stator;
- provision of a thin film of oil to seal off the gap between the moving vanes and the inner surfaces of the stator; and
- dissipation of the heat from the pump oil through the pump stator to the atmosphere which is generated from the surface frictions among moving parts and the gas compression [13].

Hence, the pump oils for oil-sealed rotary vacuum pumps must meet the following essential function requirements: a suitably low vapour pressure, a good thermal stability up to 100°C, a good spreadability to seal the moving surfaces in the pump, a good lubrication capability for the moving parts, a good chemical resistance to react with the pumped gases and oxygen, and so forth.

Commonly, three types of pump oils, namely mineral oil, white oil and synthetic oil, are used in rotary pumps.

Mineral oils are the by-products of the distillation of petroleum and are also called hydrocarbon oils and are obtained directly from petroleum refineries. The composition of these kinds of oil is predominately alkanes with trace amounts of aromatics and heterocyclics. They exhibit good lubricating properties and allow the attainment of low ultimate pressures. However, their chemical resistance is relatively poor, particularly to vigorous oxidants. As a result, mineral oils are very suitable for general-purpose use in vacuum pumps.

The technical white oil series of hydrocarbon fluids are further distilled from petroleum stocks that are processed to remove aromatics, heterocyclics and olefinic materials. As a result of removing these substances, they exhibit a good chemical reaction resistance and can be used for pumping corrosive gases and vapours such as halogens, hydrogen halides, Lewis acids ($AlCl_3$, $FeCl_3$, BCl_3 etc.) and halogencarbons. Their service lives are increased by two to three times compared with the normal mineral oils or doublystilled oils. However, this kind of hydrocarbon oil is subject to reaction with oxygen.

Synthetic pump oils are also called inert oils. So far, there are mainly two types of synthetic pump oils available: perfluoropolyethers (PFPE) and polychlorotrifluorethylenes (CTFE). PFPE oils are not flammable and inert to most gases and by-products of CVD processes. They are stable and most useful in highly

Table 2.6. Comparison of three different kinds of pump oils [7, 12]

	Mineral oil	Technical white oil	Perfluoropolyether
Resistance to halogens and halogen compounds	Low	Medium	High
Temperature resistance	Medium	Low	High
Resistance to oxidation	Medium	Low	High
Wetting properties	High	High	Low
Solvent power for abraded parts	High	Medium	Low
Minimal dwell period of reactive gases in sealant	Low	Medium	High
Resistance to Lewis acids	Low	Low	Medium
Solvent power for SiO_2	Low	Low	Low
Solvent power for NH_4Cl	Low	Low	Low
Solvent power for silicon-nitrogen compounds	High	Low	Low

corrosive environments and in the presence of large quantities of oxygen. Although PFPE oils do not react with most processing gases, many gases are highly soluble in the oils. Therefore, filtering and neutralisation techniques must be used to remove the soluble gases to prevent the acids attacking the pump parts. The main limitations of PFPE oils are their high cost and ease of decomposition by ammonia and aluminium chloride. Another problem of PFPE oils is their relatively high vapour pressure. CTFE oils share many of the properties of PFPEs, but they are much less expensive. They are stable in the presence of oxygen, halogens, hydrogen and halides; however, they are also easily decomposed by ammonia and aluminium chloride.

To summarise the performance of the three aforementioned oils, Table 2.6 has been compiled to compare and contrast these oils for CVD purposes.

As oils may react with exhaust gases and trapped soluble substances, they can produce corrosive substances and particles inside the pump will eventually cause damage to the pump. It is therefore necessary to change the oils regularly to achieve their maximum designed life. Otherwise, they may increase the mechanical wear of moving parts, leading to higher expenditures on repair and maintenance and lower efficiency in vacuum generation. When frequent oil changes are required to maintain oil quality and vacuum generation efficiency, it is necessary to consider the introduction of partial-flow or full-flow type filters (Figure 2.9). A partial-flow filter, also called a bypass filter, returns filtered oil directly to the reservoir of the pump system. The oil used to lubricate the pump is directly

pumped from the reservoir, which may contain untreated oil. This can potentially cause wear and corrosion if the untreated oil contains particles or chemically reactive substances. With a full-flow system, the filter treats the oils from the reservoir pumped by an oil pump within the vacuum pump. Purified oil is then introduced into the pump to perform its three functions. The oil filters work on either physical or chemical principles. The former uses porous filters to remove very small particles, whereas chemical filters use activated alumina to adsorb high molecular weight compounds. Activated alumina filters also act as a mechanical filter to remove particles with size down to 3 μm.

2.2.3.3 Roots Pump

In some applications a flow throughput is required to rapidly extract the gas from a chamber. In order to achieve this two methods can be employed: to increase the volume pumped on each stroke by making a bigger pump or to increase the pump rotation velocity. The former will lead to higher cost. The latter is subject to the limitations of heat dissipation within the pump and the rotation speed of the vane pumps, which is normally less than 2000 r mp. Alternatively, one can construct a pump without sliding seals. This allows very high rotational velocities because the mechanical contact friction between the vanes and the walls of the stator does not exist. Compression is achieved by using a narrow clearness between the rotating parts and the walls. In the simplest case this can be used as precompressor for a conventional rotary pump. This kind of vacuum pump is named after its inventor – the brothers Philander and Francis Roots, who patented their design in 1860.

The working principle of the Roots pump is shown in Figure 2.10. It consists of two impellers constructed in a shape of Arabic numeral eight (figure 8). These impellers are rotated in opposite directions within the pump housing. The shaft of the driving impeller is directly connected to a motor or via a belt, whereas the shaft of the driving impeller is normally connected to gears and rotates in the opposite direction. When one of the impellers is at its vertical position as shown in Figure 2.10a, its bottom surface is tangential to the middle section surface of the other impeller, which is in a horizontal orientation. This arrangement of the impellers ensures the isolation of the inlet from the exhaust outlet. When the top impeller rotates further to the horizontal orientation with the bottom impeller in a vertical
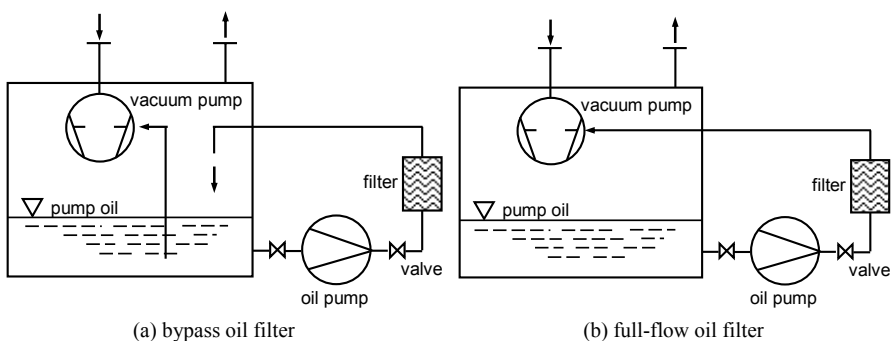

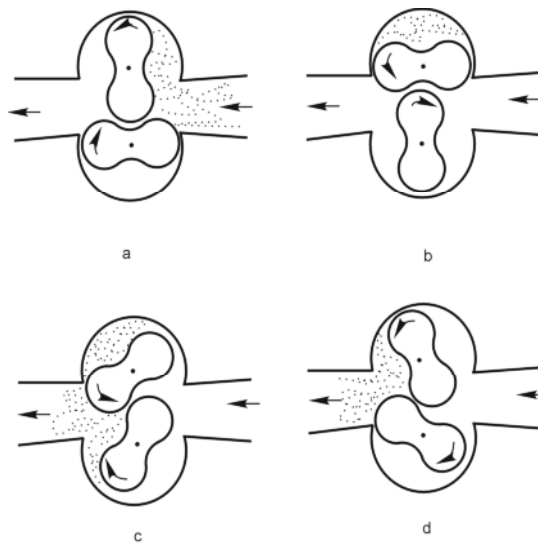**Figure 2.9.** Schematic of oil filtration system for oil-sealed rotary pumps [7]

Figure 2.10. Working principle of Roots pump [3]

position as shown in Figure 2.10b, the gas withdrawn into the top chamber is separated from the inlet channel and forced into the exhaust outlet. A further rotation by the top impeller forces the gas into the exhaust outlet as the bottom impeller seals off the bottom half of the impeller housing, shown in Figure 2.10c. For every rotation by the top impeller, there are two cycles of gas pumping actions, in other words, twice as much as the gas shown in the shaded area in Figure 2.10b is pumped or forced through the Roots pump system.

The Roots pump is always connected to a mechanical pump, which provides a second-stage pumping between it and the atmosphere. The pressure difference
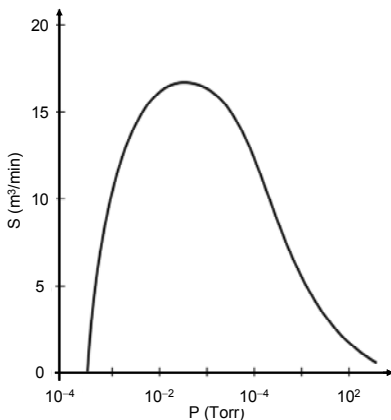
Figure 2.11. Typical pumping velocity curve of a Roots pump [3]

across a typical Roots pump is much less than 760 Torr. Because the oil usually creates undesirable vapour pressure, it is not necessary for sealing the clearance ($\sim 10^{-1}$ mm) between two impellers and impeller/housing. Oil is only used to lubricate the gears, which ensures the very accurate synchronisation of the rotors. The results shown in Figure 2.11 indicate that a Roots pump is suitable for high velocity pumping in the pressure range of 10^{-2} to 10 Torr. Maximum efficiency occurs when the pump is operated at a compression ratio of about 10 at a pressure on the order of 5×10^{-2} Torr; thus the pump must be connected to and backed by a suitable mechanical pump.

As there is no oil sealing for Roots pumps, the impellers have to be designed and manufactured with a close fitness between them and the pump housing. The profiles of the two impellers are designed not to touch each other, nor do they touch the internal surface of the housing when the impellers are rotating. To ensure minimum gas leakage or back flow from the compressing region to other areas, the clearance caused by the geometry definition and the tolerances of the impeller profile has to be very small, usually about 0.1 to 0.5 mm between these surfaces. This design thus ensures that the inlet port is almost isolated from the outlet port. The small clearance between parts causes a small back flow of gas from the exhaust port to the inlet port. Accordingly, the efficiency of compression is much lower than that of oil-sealed pumps. However, the essential design requirements here are the high throughputs generated by high pumping speed. The avoidance of rubbing and sliding contacts between the propellers and the housing allows much higher velocities of rotation in the range of 1400 to 4000 rpm as against the highest speed of 2000 rpm for mechanical pumps, and consequently much higher pumping speed.

2.2.4   Vacuum Measurement and Leak Detection

With the above introduction to the vacuum generation technologies, it is also important to accurately measure and to detect the level of the vacuum within a chamber. This section introduces the basic working principles of these devices covering the most common CVD systems.

2.2.4.1 Vacuum Measurement

As mentioned before, the vacuum pressure covered in current vacuum technologies is about 19 orders of magnitude from 10^{4} Pa (rough vacuum) to 10^{-15} Pa (outer space vacuum). It is impossible to measure the pressure with a single pressure gauge over the whole vacuum range. Consequently, a series of vacuum gauges have been designed and developed, and they fall into two groups: direct measurement (e.g. mechanical phenomena gauges) and indirect measurement (i.e. transport phenomena gauges and ionisation gauges).

The mechanical phenomena gauges measure the actual force exerted by the gas. They include a U-tube, a capsule dial, a strain, a capacitance manometer, a McLeod gauge, etc. Vacuum is measured according to the displacement of an elastic material or by measuring the force required to compensate its displacement. The measurement ranges from atmospheric pressure to 10^{2} Pa in rough vacuum conditions.
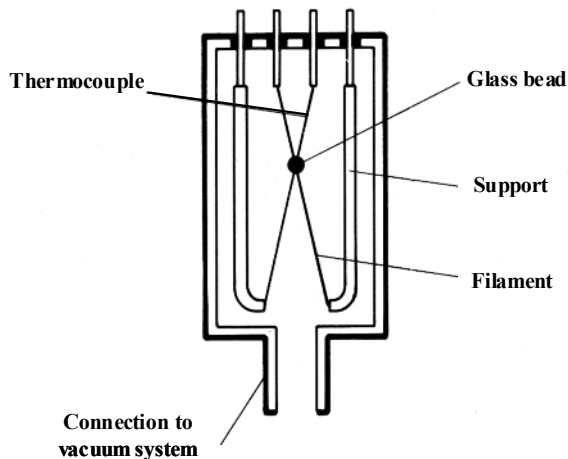
Figure 2.12. Measure principle of thermocouple gauge [10]

The thermocouple gauge is a typical indirect measurement device in a CVD system, and its working principle is as shown in Figure 2.12. The filament is heated by electric current with a constant power. The thermocouples are connected with the filament by a small glass bead, which ensures thermal contact rather than electric contact. In such a case, the temperature of the heated filament is measured by the thermocouple. According to the state equation of perfect gases, the amount of molecules is proportional to the pressure within a chamber. If the pressure is high, the collision frequency between the molecules and the heated filament is also high. Therefore, a high flux of the heat is transferred away from the heated filament. If the pressure is decreased, there are fewer molecules to take away the heat from the filament. The pressure within the vacuum chamber can be indirectly measured by the temperature. At relatively low pressure, the heat transfer from the hot to the cold surface (Q) is proportional to the pressure and is given by [3]

$$Q = \frac{\alpha}{2} \cdot \frac{Pu_{av}(T_s - T_i)}{T_i}$$

(2.29)

where α is the accommodation coefficient, P is the pressure, u_{av} is the average velocity of the gas at the temperature T_i, and T_s is the temperature of the hot surface.

2.2.4.2 Leak Detection

Creating a required vacuum in a reaction chamber is the first step in any CVD process. Maintaining the required level of vacuum is the next important task. An important aspect of maintaining the required vacuum is avoiding or minimising any leakage of external gases. It is inevitable to have some level of leakage as it is impossible to manufacture a 100% sealed system, due to various manufacturing constraints and tolerances, mechanical wear and the requirements of dynamic gas circulation within a system. As long as the leakage is within acceptable levels, a
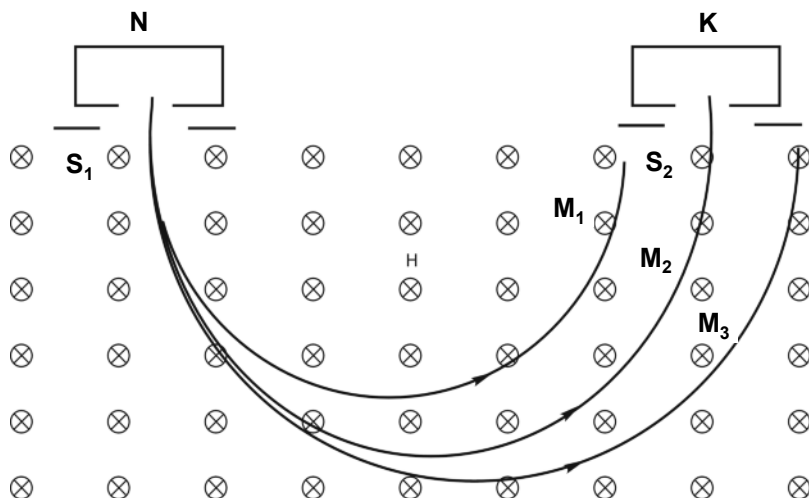
Figure 2.13. Schematic of helium-specific mass spectrometer leak detector
H: uniform magnetic field; N: ionisation chamber; K: ion collector, S_1: entrance of ions,
S_2: exit of ions

CVD operation can still produce satisfactory products. It is therefore important and essential for the system to be able to detect the leakage occurring before and during a CVD operation. Once an acceptable level of leakage is maintained, a CVD process may commence. If there is an unacceptable level of leakage, it can cause a severe problem for the CVD process and the quality of the deposit.

There are normally two types of leakage detection systems, namely halide leak detector and helium-specific mass spectrometer leak detector, based on the types of gases to be detected. As CVD systems usually use large quantities of halides as reactant precursors, there are normally some residual halides within the reaction chamber. This consequently influences the accuracy of the halide leak detector. In this case, helium-specific mass spectrometer leak detectors are normally used to avoid this problem.

The working principle of a helium-specific mass spectrometer leak detector is as follows [7]. The mass spectrometer mainly consists of three parts: an ion source, a deflection system and an ion collector. When the atoms pass the ionisation chamber of the detector, they are ionised to become positive ions. When these ions are then accelerated in the ionisation chamber, they obtain sufficient energy and enter into the magnetic field of the detector. These positive ions travel in a specific orbit in the magnetic field. As different ions have specific orbit radii; only ions with the same orbit radius as that of the spectrometer can pass a narrow gap, as indicated by K in Figure 2.13, and reach the ion collector K to form an ion stream.

Under the influence of a homogeneous magnetic field, perpendicular to the path of the ions, they are deflected into circular orbits of a radius given by

$$r = \frac{1}{B}\sqrt{\frac{2mV}{ze}} \qquad\qquad (2.30)$$

where m is the mass of ion in kilograms, V is the ion-accelerating voltage in volts, e is the electric charge in "A·s", z is the number of charges carried by the ion and B is magnetic flux density in "kg·s^{-2}·A^{-1}".

When helium is used as an indicative gas, it is possible to adjust the voltage and the intensity of the magnetic field described above such that only helium ions can reach the ion collector K in Figure 2.13 with a suitable orbiting radius. During gas leakage detection, if helium ions appear on the helium-specific mass spectrometer, it is clear that there is a leakage in the system. In the above detection process helium has been used as the detection gas for the leakage; its advantages and the reasons for such a selection are as follows:

1. there exist very small quantities of helium in the air and the residual gas in the work chamber. Therefore, it is easy to detect its presence.
2. Helium is very light and its molecule is very small, making it easy for it to pass the narrow leakage gap to reach the ion collector of a mass spectrometer, and travelling at a higher speed in the work chamber than other gases guarantees a good sensitivity of the leakage detection.
3. Helium is also an inert gas; it does not react chemically with other gases and mechanical parts, resulting in an ideal search gas which maintains its molecular quantity in the system for easy and reliable detection.

2.3   Fundamentals of Gas Transport

In CVD processes, the access of the reactant gases to the substrate surface is governed by the transport phenomena; it requires careful and timely control in order to achieve good quality and efficiency. The driving forces for the transport are the concentration gradient, pressure gradient and temperature gradients of the gases. As the gases flow, their momentum, energy and mass all vary, and therefore gas transport greatly influences not only the deposition rate but also the quality and deposition mechanism. This section discusses these key issues and aims to establish the impact of gas transport on CVD processes and the necessity of designing accurately controlled equipment for gas transport.

Momentum, thermal and mass transports are three basic physical phenomena of any fluid flow. In a CVD process, when the precursor gases enter a high temperature reaction chamber from room temperature, the aforementioned three transports occur under certain velocity, temperature and concentration gradients. The common underlying physical laws for these three transports are all based on a molecule's thermal motion. Three specific underlying laws which describe the three transports are Newton's viscous law, Fourier law and Fick's law respectively. For a simple one-dimensional system, these laws can be expressed by [14]

Momentum flux $\tau = -\mu \dfrac{du}{dy}$ (2.31)

Thermal flux $q = -\alpha \dfrac{dT}{dy}$ (2.32)

Mass flux $J = -D \dfrac{d\rho}{dy}$ (2.33)

where $\dfrac{du}{dy}$, $\dfrac{dT}{dy}$ and $\dfrac{d\rho}{dy}$ are velocity gradient, temperature gradient and concentration gradient respectively; μ, α and D are dynamic viscosity, thermal conductivity and diffusivity (diffusion coefficient) respectively.

2.3.1 Transport Coefficients

Transport coefficients are a group of coefficients used to predict the diffusivity, thermal conductivity and viscosity of gases. These in turn define the impact of the momentum, energy and mass of the gas flow. Two theories have been developed to estimate these coefficients.

2.3.1.1 Prediction from Elementary Kinetic Theory [15, 17]

Molecules move randomly in the gas state and collide with each other. They transfer momentum, energy and mass if there are gradients in their velocity, temperature and concentration. In the dilute gas region and at low pressure near atmospheric pressure, the transport coefficients can be predicted by using a kinetic theory of gases. The elementary kinetic theory (EKT) assumes all molecules to be non-interacting rigid spheres with a specific diameter, d (with mass m), moving randomly at a mean velocity, u_{av}. Using the EKT, the transport coefficients of diffusivity (D_{AB}), thermal conductivity (α) and viscosity (μ) are defined as

$$D_{AB} = \frac{1}{3} u_{av} \lambda = \frac{2}{3 p d_{AB}^2} \sqrt{\frac{k^3 T^3}{\pi^3 m_{AB}}}$$ (2.34)

$$\alpha = 2kZ\lambda = \frac{1}{d^2} \sqrt{\frac{k^3 T}{\pi^3 m}}$$ (2.35)

$$\mu = \frac{1}{3} \rho u_{av} \lambda = \frac{2}{3 d^2} \sqrt{\frac{mkT}{\pi^3}}$$ (2.36)

where ρ is the density of gas; Z is the number of molecules per unit area per unit time crossing a plane from one side; u_{av}, λ, m and d are the average velocity, mean free path, mass of one molecule and molecular diameter of gas respectively.

These equations are approximately correct because they successfully establish the relationship between the coefficients of transport with pressure and temperature. For example, the molecular diffusivity is proportional to the 3/2

power of temperature but inversely proportional to the pressure. However, both the thermal conductivity and viscosity are dependent on temperature only.

2.3.1.2 *Prediction from Chapman–Enskog Theory* [15, 17]

The forces of attraction and repulsion between molecules must be considered for a more accurate and rigorous representation of the gas flow. Chapman and Enskog proposed a well-known theory in which they use a distribution function, the Boltzmann equation, instead of the mean free path. Using this approach, for a pair of non-polar molecules, an intermolecular potential, $V(r)$, is given in the potential function proposed by the Lennard–Jones potential:

$$V(r) = 4\varepsilon[(\frac{\sigma}{r})^{12} - (\frac{\sigma}{r})^6] \tag{2.37}$$

where r is the radial distance between the two molecules, σ is the collision diameter determined from quantum mechanics and ε is the characteristic energy.

Based on these, more accurate expressions to calculate the coefficients are obtained. The detailed deviations of these coefficients can be found in the references [18, 19]; the results are given as follows.

The diffusivity D_{AB} is given by

$$D_{AB} = \frac{0.00188}{P\sigma_{AB}^2 \Omega_{D,AB}} \sqrt{(\frac{1}{M_A} + \frac{1}{M_B})T^3} \quad (\text{cm}^2 \cdot \text{s}^{-1}) \tag{2.38}$$

where P is the pressure in atmospheric pressure, T is the temperature in Kelvin, σ_{AB} is the characteristic length in angstrom, $\Omega_{D,AB}$ is the diffusion collision integral, dimensionless, and M_A and M_B are the mole masses of gases A and B in g·mol^{-1} respectively.

The viscosity μ is expressed by

$$\mu = \frac{26.69}{\sigma^2 \Omega_\mu} \sqrt{MT} \quad (\mu\text{Pa·s}) \tag{2.39}$$

where M is the mole mass in garms per mole, T is the temperature in Kelvin, σ is the collision diameter in angstrom, and Ω_μ is the viscosity collision integral, dimensionless.

The thermal conductivity α is presented as

$$\alpha = \frac{2.63 \times 10^{-23}}{\sigma^2 \Omega_\alpha} \sqrt{\frac{T}{M}} \quad (\text{W·m}^{-1}\cdot\text{K}^{-1}) \tag{2.40}$$

where M is the mole mass in kilogarms per mole, T is the temperature in Kelvin, σ is the collision diameter in meters, and Ω_α is the thermal conductivity collision integral, dimensionless.

Unlike the elementary kinetic theory, the three collision integrals ($\Omega_{D,AB}$, Ω_μ and Ω_α) are introduced in the Chapman–Enskog theory. Moreover, the collision diameter (σ) is used instead of the molecular diameter (d).
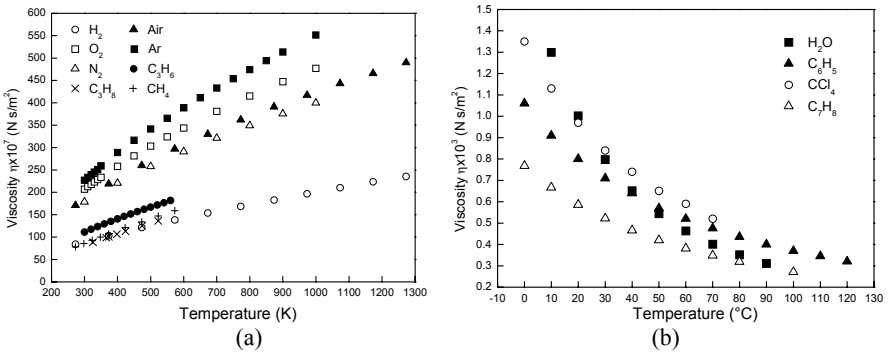
Figure 2.14. Relationship between viscosity of various fluids and temperature, data from [21]: (a) for gases and (b) for liquids

It is interesting to note that the viscosity of gas is independent of pressure and increases with temperature, whereas in the case of liquids the viscosity is known to decrease as the temperature increases [20]. The temperature dependence of viscosities for the gases and the liquids are shown in Figure 2.14a and b respectively. This difference in the effect of temperature on the viscosity of liquids and gases can be explained by structural differences between liquids and gases. In liquids, molecules exert strong cohesive forces between molecules as they are closely arranged spatially. The intermolecular forces determine the relative motions between adjacent layers of a fluid. As the temperature increases, molecules become more active and the intermolecular cohesive forces are reduced, implying a reduction in interlayer resistance to motion. As the viscosity is a measure of internal friction or resistance within fluids, the viscosity is therefore reduced by an increase in temperature as a result of the reduction of the intermolecular cohesive forces. However, the gas molecules are spaced so widely that their intermolecular forces become negligible. When the gas temperature increases, their resistance increases due to the fact that more molecules are colliding with each other, resulting in higher resistance for the molecules to move in an intended direction. In contrast to the liquids, the viscosity of gases increases as the temperature rises, caused by the random molecular collision and momentum exchange.

Example:

Calculation of the diffusivity for CH_4 in N_2 at 20°C and 1 atm.

In order to use Equation (2.39), it is necessary to compute the values of the collision diameter, σ_{AB}, and the collision integral, Ω_D. The collision integral, in turn, depends on the parameter KT/ε. The individual values for gas A–CH_4 and gas B –N_2 can be found in the tables in [14–17]:

$$M_A = 16.04, \ \sigma_A = 3.822 \text{ Å}, \ \varepsilon_A/K = 137 \text{ K} \tag{2.41}$$

$$M_B = 28.02, \sigma_B = 3.681 \text{ Å}, \varepsilon_B/K = 91.5 \text{ K} \tag{2.42}$$

The parameters σ_{AB} and ε_{AB} for the collision of CH_4 with N_2 may be estimated by means of the following equations:

$$\sigma_{AB} = \frac{\sigma_A + \sigma_B}{2} = \frac{3.822 + 3.681}{2} = 3.752 \text{ Å} \tag{2.43}$$

$$\varepsilon_{AB}/K = \sqrt{\varepsilon_A \varepsilon_B} = \sqrt{137 \times 91.5} = 111.96 \tag{2.44}$$

$$KT/\varepsilon_{AB} = 293/111.96 = 2.617 \tag{2.45}$$

Interpolating the values of collision integrals found in the tables in [14–17]: we obtain a value for the collision integral of CH_4 and N_2, $\Omega_D = 0.9860$, and then the substitution of the foregoing values into Equation (2.38) gives

$$D_{AB} = \frac{0.00188}{1.0 \times (3.752)^2 \times 0.9860} \sqrt{(\frac{1}{16.04} + \frac{1}{28.02}) \times 293^3} = 0.21 \text{ cm}^2\text{s}^{-1}$$
$$\tag{2.46}$$

2.3.1.3 Transport Coefficients in Multicomponent Gas Mixtures

This rigorous theory developed by Chapman and Enskog can also be used to calculate the transport coefficients of multicomponent gas mixture. For a diluent gas mixture, the diffusivity of the diluent component (i) into a homogeneous gas mixture (D_{im}) is given by [15]

$$D_{im} = (\sum_{\substack{j=1 \\ j \neq i}}^{n} \frac{x_j}{D_{ij}})^{-1} \tag{2.47}$$

where D_{ij} is the binary diffusivity of the ij gas system and x_j is the mole fraction of the jth gas in the gas mixture.

Under conditions of low pressure, the viscosity expression of the multicomponent mixture is much more complex. It is usual to use two simple methods which were developed by Wilke as well as Herning and Zipperer.

In Wilke's approach, the second-order effects are neglected and the final expression of the viscosity is given by [15, 22]

$$\mu_m = \sum_{i=1}^{n} \frac{y_i \mu_i}{\sum_{j=1}^{n} y_j \Phi_{ij}} \tag{2.48}$$

where μ_m is the viscosity of the multicomponent gas mixture, μ_i is the viscosity of the pure ith gas, y_i is the mole fraction of the ith gas in the mixture and Φ_{ij} is the interacting parameter for gas mixture viscosity and given by [15]

$$\Phi_{ij} = \frac{[1 + (\mu_i / \mu_j)^{1/2} (M_j / M_i)^{1/4}]^2}{[8(1 + M_i / M_j)]^{1/2}}$$

(2.49)

$$\Phi_{ji} = \frac{\mu_j}{\mu_i} \frac{M_i}{M_j} \Phi_{ij}$$

(2.50)

where μ_i and μ_j are the viscosities of the pure ith and jth gases respectively; M_i and M_j are the mole masses of the ith and jth gases respectively.

In Herning and Zipperen's approach, the relationship between Φ_{ij} and Φ_{ji} is much simpler than that of the method proposed by Wilke. The expression is written as [15, 23]

$$\Phi_{ij} = (\frac{M_j}{M_i})^{1/2} = \Phi_{ji}^{-1}$$

(2.51)

At relatively low pressure, the thermal conductivity of a gas mixture, α_m, is presented as follows [15, 24]:

$$\alpha_m = \sum_{i=1}^{n} \frac{y_i \alpha_i}{\sum_{j=1}^{n} y_i A_{ij}}$$

(2.52)

where α_i is the thermal conductivity of the pure ith gas. A_{ij} is a function for the gas mixture thermal conductivity and is equal to Φ_{ij} in Equation (2.51).

2.3.1.4 Diffusion of Gases in Porous Media [25, 26]
Gas diffusion in a porous structure is of particular interest to this book as many porous fibre preforms are densified by CVI. The diffusion of gases in porous media can be classified into three regimes according to the ratio of the free mean path to the pore diameter within the structure. As shown in Figure 2.15, they are Fick gas diffusion, transition gas diffusion and Knudsen gas diffusion.

Fick diffusion takes place when the pore diameter is much greater than the mean free path of the molecule. In this case, the collisions between the molecules dominate and the collision between the molecule and the walls of the pore is negligible in Figure 2.15a. The driving force of the Fick diffusion is the concentration gradient of the gaseous species and the diffusivity discussed above.
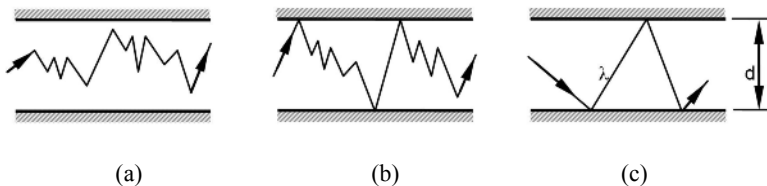

(a)   (b)   (c)

Figure 2.15. Gas diffusion types within a pore: (a) fick diffusion, (b) transition diffusion and (c) Knudsen diffusion

If the pore diameter is comparable to the mean free path of the molecules, the collision between the molecules and the walls of the pore becomes dominant in Figure 2.15c. The mass transport is determined by the Knudsen diffusion. In such a case, the Knudsen diffusion occurs in the small channels among the fibres within the fibre bundle of the preform. When the mean free path λ is intermediate in length between the above two limits, the transition diffusion happens as shown in Figure 2.15b.

The Knudsen diffusivity is calculated from the following expression:

$$D_K = \frac{2}{3} r u_{av} \tag{2.53}$$

where D_K is diffusivity in square metres per second, r and u_{av} is the average pore radius in meter and molecular velocity for the gaseous component A in metres per second. By using the kinetic theory of gases, D_K is rewritten as

$$D_K = 97.0 r (\frac{T}{M_A})^{1/2} \tag{2.54}$$

where M_A is the molecular mass of A and T is temperature in Kelvin.

The Knudsen diffusivity is proportional to the radius of the pore and the temperature but inversely proportional to the mole mass of the gas. This implies that small gaseous species exhibit high diffusivity. Unlike the Fick diffusivity, the Knudsen diffusivity is independent of pressure.

For the transition-type diffusion, the efficient diffusivity (D_e) is given by

$$\frac{1}{D_e} = \frac{1}{D_F} + \frac{1}{D_K} \tag{2.55}$$

2.3.1.5 Permeability

Permeability is a parameter defined to measure the physical influence of a porous structure on fluid flow, and for a CVI process it is an important physical parameter for fibre preforms. Another important parameter for porous structure is the porosity, which is the most important geometrical property. According to Darcy's law, the volumetric flow rate Q of a fluid through a porous medium is proportional to the hydrostatic pressure difference (ΔP) across the structure (see Figure 2.16) , the permeability and the cross-section area, and is also inversely proportional to the length of the structure and the viscosity of the fluid, as given by [26]
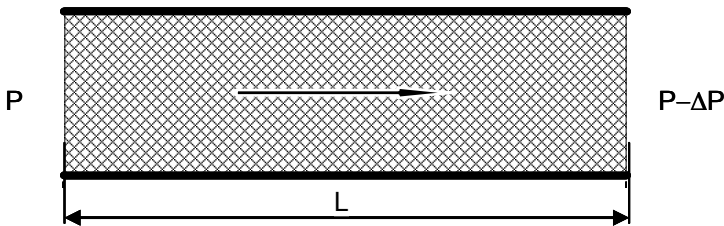

Figure 2.16. Fluid flow through a porous medium

$$Q = \frac{\kappa A \Delta P}{\mu L} \tag{2.56}$$

where A and L are the normal cross area and the length of the porous structure, κ is the permeability of the porous structure and μ is the dynamic viscosity of the fluid.

To understand this permeability, many investigations have been undertaken and empirical relationships have been established. Following Tai and Chou [27], the empirical expression for the local permeability distribution is adopted for the fibre preform. Permeability is thus obtained as

$$\kappa = \frac{\pi d^2 \ln[0.64/(1-\phi)^2]}{24.4} \frac{\phi}{1-\phi} \tag{2.57}$$

where d is the diameter of the fibre and ϕ is the porosity of the preform. Within a unit cell of fibre preform, the local porosity of a unit cell can be expressed as

$$\phi = 1 - \frac{(9.928L - 23.659r)\pi r^2}{L^3} \tag{2.58}$$

where L is the length of the unit cell and r is the radius of the fibre.

2.3.2 Boundary Layer Theory

The boundary layer theory is very important for understanding the transport phenomena and the growth kinetics of a CVD coating. It was proposed to address the questions that neither theoretical hydrodynamics nor experimental hydraulics could explain well in the past. At the end of the 19th century fluid mechanics studies were dominated by two distinctively different schools of thought which had nothing in common [28]. The science of theoretical hydrodynamics, evolved from Euler's theory for ideal frictionless and non-viscous liquids, was developed to a high degree of completeness. However, the hydrodynamic theory could not explain some experimental results such as the pressure losses in pipes and drag force. Based on its frictionless assumption, one famous deduced paradoxical example, the so-called Alembert Paradox, states that a body moving through a uniform fluid which extends to infinity experiences no drag or force acting in the opposite direction of its motion. This obviously is not the case and hence this school of thought became useless for addressing practical engineering problems, as many important practical flow problems could not be solved.

For this reason, practical engineers developed their own highly empirical understanding of hydraulics which appeared to be more pragmatic and effective in solving important practical engineering problems. The hydraulics was developed on the basis of a large number of experimental tests; however, the methods differed greatly from each other, making the results difficult to generalise into theory-based knowledge.

The boundary layer theory was first developed by Ludwig Prandtl in 1904. The theory points out that the fluid flow along the surface of a body is divided into two regions: the boundary layer and the flow outside the boundary layer.

The boundary layer is a thin fluid film that forms on the surface of a solid body moving through a viscous fluid. The majority of the drag force experienced by the moving body which is immersed in a fluid is due to viscous shear and inertial forces within the boundary layer;

The flow outside the boundary layer is determined by inertial forces only. Shear forces and the viscosity of the fluid within the boundary layer can be neglected without significant effects on the solution.

The boundary layer theory reconciles the important contradictions between experimental hydraulics and theoretical hydrodynamics. It effectively combines both approaches into an integrated theory.

The thickness of the velocity boundary layer is normally defined as the distance from the solid body to the fluid layer at which the flow velocity reaches 99% of the free stream velocity, as illustrated in Figure 2.17. For a flat-plate body emerging in an incompressible and laminar fluid, the boundary layer thickness is given by

$$\delta = \frac{5.0}{\sqrt{Re}} x \tag{2.59}$$

where x is the distance from the leading edge of the plate and Re is the Reynolds number of the flow.

The velocity boundary layer concept can be extended to define the temperature and concentration of a fluid. The temperature boundary layer thickness is the distance from the body to a layer at which the temperature is 99% of the temperature from an inviscid solution. The boundary layer thickness for the fluid concentration has the same definition. Their relationships are expressed by [29]

$$(T_S - T)/(T_S - T_\infty) = 0.99 \tag{2.60}$$

$$(C_S - C)/(C_S - C_\infty) = 0.99 \tag{2.61}$$

The boundary layer theory has been widely accepted and used to describe the transport phenomena in CVD processes. High-performance CVD systems require designers to focus on the geometrical parameters of the reaction chamber, the orientation and arrangement of the preforms in the chamber, as well as some other important components, such as pipes, distributor, exit and so forth. Due to drag effects around the boundary layer of preforms, it is very important to design the preforms and the reaction chamber and aim to avoid the boundary layer separation such that they experience a minimum drag force. The details of these effects are discussed in Chapter 6.
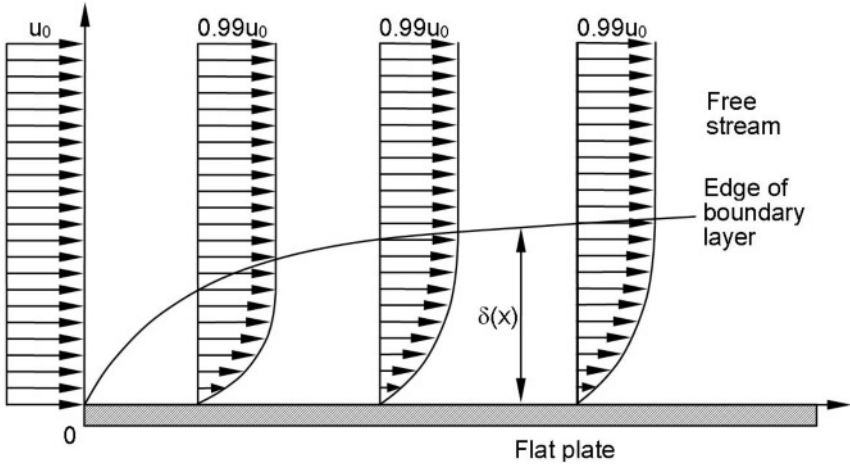
Figure 2.17. Profile of a boundary layer along a flat plate

2.3.3   Some Dimensionless Parameters

Having introduced some theoretical and empirical developments, it is also important to introduce several dimensionless parameters. These parameters could basically characterise the transport processes of gases.

2.3.3.1   Knudsen Number [25, 30]
A fluid is usually considered as a continuous substance under normal conditions. In fact, it is composed of myriads of continuously moving molecules. For gases at 1 atm, 25°C, the spacing between molecules is on the order of 10^{-3} μm, and for the liquids it is on the order of 10^{-4} μm. The number of molecules per cubic micrometer is 2.69×10^7 for air and 3.21×10^{10} for water. Hence, it is reasonable to assume and treat the fluid as a continuum.

The Knudsen number (Kn) is used to determine the different regimes of the gas flow. These regimes can be divided into continuous flow, transitional flow and free molecular flow. This division is based on the understanding that the flow behaviour differs within each of the flow regimes. The Knudsen number is defined as

$$Kn = \frac{\lambda}{L} = \frac{kT}{\sqrt{2}\pi d^2 PL} \tag{2.62}$$

where λ is the mean free path, L is the characteristic length, k is Boltzmann's constant, T is the temperature, d is the molecular diameter and P is the total pressure.

When $\lambda \ll L$ or $Kn \ll 0.01$, many collisions between molecules occur, hence the gas can be regarded as a continuum. Under this condition or regime, the flow of
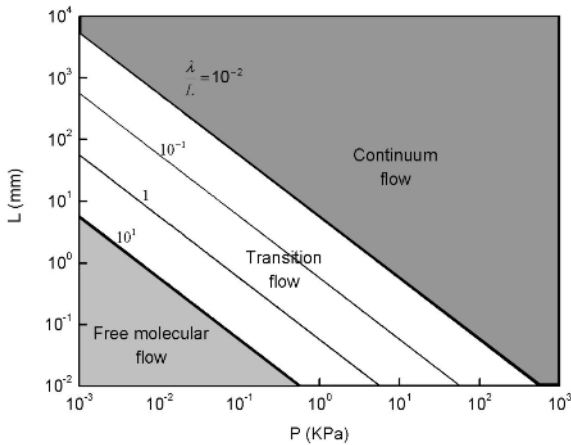
Figure 2.18. Map of different flow regimes of H_2

the gases can be described by the Navier–Stokes equation. Such conditions are fulfilled in the rough vacuum range of some CVD processes. The next regime is called transition regime, where $0.01 < Kn < 10$. Within this regime, it is very difficult to establish a theoretical model at the present time. In high and ultra-high vacuum conditions, λ is significantly greater than L, that is $Kn > 10$. This regime corresponds to the free molecular flow in which the wall collisions dominate and the molecules undergo few collisions with each other.

The detailed flow regime flow map for hydrogen gas is shown in Figure 2.18. For the CVI techniques discussed in Chapter 5, the process is usually performed at a pressure of 10 to 30 kPa. The gas flow can be treated as continuum flow if the characteristic length is more than 1 mm.
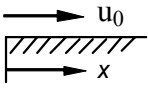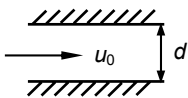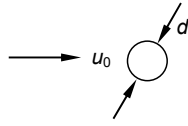
2.3.3.2 Reynolds Number [14, 20]
The Reynolds number is undoubtedly the most famous dimensionless parameter in fluid mechanics. It is named in honour of Osborne Reynolds, a British engineer who first demonstrated in 1883 that a dimensionless variable can be used as a criterion to distinguish the flow patterns of a fluid either being laminar or turbulent. Typically, a Reynolds number is given as follows:

$$\mathrm{Re} = \frac{\rho u L}{\mu} = \frac{u L}{\nu} \tag{2.63}$$

where u is the mean fluid velocity, L is the characteristic length, ρ is the density of a fluid, and μ and ν are the dynamic viscosity and kinematic viscosity of a fluid respectively. Their relationship is given by

$$\nu = \frac{\mu}{\rho} \tag{2.64}$$

Table 2.7. Characteristic velocity and length for three flow cases

Flow type	Flow over a flat plate	Flow in a pipe	Flow around a cylinder
Characteristic velocity	Stream velocity (u_0)	Mean velocity within the pipe (u_0)	Remote velocity of flow (u_0)
Characteristic length	Distance measured from leading edge of plate (x)	Diameter of pipe (d)	Diameter of cylinder or sphere (d)
Critical Re	5×10^5	2100	3×10^5

In fluid mechanics, the physical implication of a Reynolds number is the ratio of inertial forces ($u\rho$) to viscous forces (μ/L). It is, therefore, used to illustrate the relative importance and dominance of these two types of forces for a given flow. Depending on the magnitude of the Reynolds number, the flow regimes can be classified as either laminar or turbulent flow. If a flow has a low Reynolds number, a laminar flow occurs, where viscous forces are dominant. The flow is therefore smooth. When the Reynolds number for a flow is greater than a critical value, the flow becomes turbulent flow and is dominated by inertial forces, resulting in random eddies, vortices and other flow fluctuations. Some of the examples are illustrated in Table 2.7.

Most CVD reactors operate in the laminar regime ($Re < 100$) due to the low precursor flow rate [31, 32].

2.3.3.3 Grashof Number [14]

The Grashof number plays the same role in free convection as the Reynolds number plays in forced convection. The Reynolds number provides a measure of the ratio of the inertial to viscous forces acting on a fluid. By contrast, the Grashof number is a ratio of the buoyancy force to the viscous force acting on a fluid. It is named after the German engineer Franz Grashof and the expression is given by

$$Gr = \frac{g\beta\Delta TL^3}{v^2} \tag{2.65}$$

where g is the gravitational acceleration, L is the characteristic length, ΔT is the temperature difference, β is the volume thermal expansion coefficient of a fluid and v is kinematic viscosity.
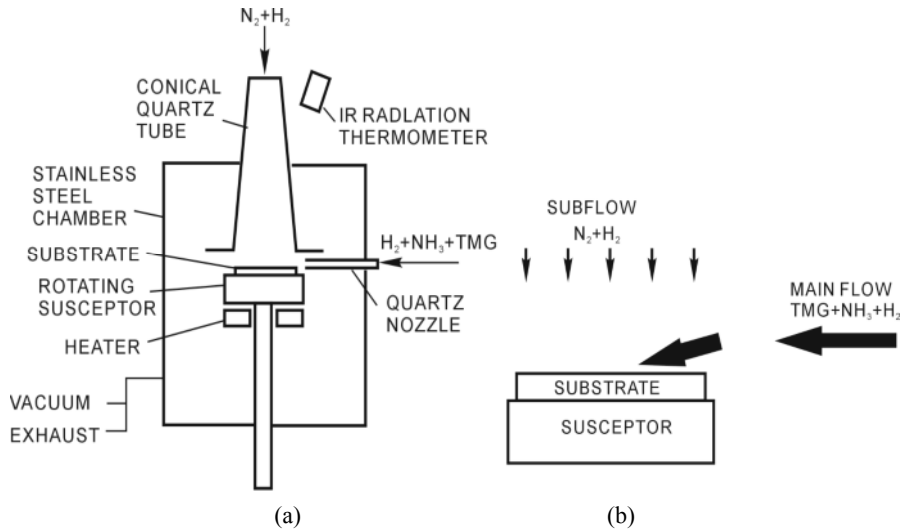
Figure 2.19. Design of gas flow for MOCVD GaN [36]: (a) schematic of MOCVD chamber and (b) flow directions of the gases

The Grashof number is a dimensionless parameter used to analyse the flow patterns of a fluid. When the *Gr* number is much greater than 1, the viscous force is negligible compared to the buoyancy forces. When buoyant forces overcome viscous forces, the flow starts a transition to the turbulent regime [28, 34]. For a flat plate in vertical orientation, this transition occurs at a *Gr* number of around 10^9.

It is clear that the free convection flow becomes significant with an increase in the temperature difference and characteristic length. A large CVD reactor possesses a large characteristic length. For a CVD process, free convection flow is always undesirable because it is uncontrollable [35, 36]. A good example is the MOCVD reactor design for GaN thin-film deposition proposed by Nakamura as shown in Figure 2.19. If the precursor gases of H_2-NH_3-TMG are only delivered parallel to the sapphire substrate, it is impossible to obtain the continuous GaN film. When another subflow of N_2-H_2 gas flow is introduced perpendicular to the reactant precursor gas flow, the inert subflow of H_2-N_2 forces the reactant gases to flow towards and closer to the substrate, rather than flow away from the substrate surface due to free convection. This allows high-quality GaN film to be successfully deposited.

2.3.3.4 *Prandtl Number*[14, 25]

The Prandtl number is a dimensionless number named after Ludwig Prandtl. It is defined as the ratio of momentum diffusivity (kinematic viscosity) to the thermal diffusivity, as well as the ratio of viscous diffusion rate to thermal diffusion rate:

$$\Pr = \frac{v}{\alpha} = \frac{C_p \mu}{k} \tag{2.66}$$

where Cp is the specific heat, α is the thermal conductivity, k is the thermal diffusivity, v is the kinematic viscosity and μ is the dynamic viscosity.

The ratio of the velocity boundary layer (δ) to temperature boundary layer (δ_T), as discussed in Section 2.3.2, is governed by the Prandtl number. If the Prandtl number is 1, the two boundary layers have the same thickness. If the Prandtl number is greater than 1, the thermal boundary layer is thinner than the velocity boundary layer. If the Prandtl number is less than 1, which is the case for CVD reactant gases under standard conditions, the thermal boundary layer is thicker than the velocity boundary layer. The relationship between the velocity boundary layer (δ) to temperature boundary layer (δ_T) is given by

$$\frac{\delta}{\delta_T} = Pr^{1/3} \tag{2.67}$$

The Prandtl numbers of gases (such as H_2 and Ar) commonly used in the CVD processes are around 0.7. Accordingly, the velocity boundary layer is just slightly thinner than that of the thermal boundary layer. For liquid metals (e.g. mercury) with small Prandtl numbers and low viscosities, the thickness of the velocity boundary layer is much thinner that of the thermal boundary layer. For oils with large Prandlt numbers and high viscosities, the thickness of the thermal boundary layer is one order less than that of the velocity boundary layer, as shown in Figure 2.20.

The Prandtl values for some fluids are listed in Table 2.8. For mercury, heat conduction is more effective compared to convection when thermal diffusivity is dominant. For engine oil, convection is very effective in transferring energy from an area, compared to pure conduction, where the momentum diffusivity is dominant. In heat transfer problems, the Prandtl number controls the relative
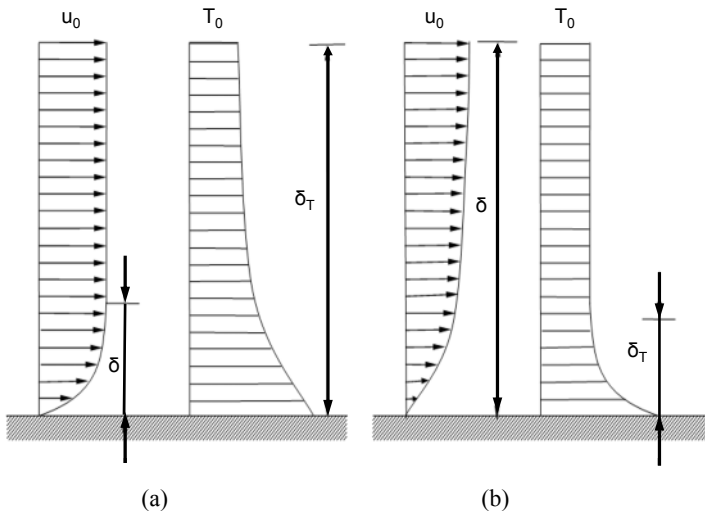

Figure 2.20. Comparison of boundary layers between the different fluids: (a) Pr→0 (for liquid metal) and (b) Pr→∞ (for viscous oil)

Table 2.8. Pr values for different fluids

Fluid	Air	H_2	He	N_2	Water	Engine oil	Mercury
Pr	0.7	0.71	0.7	0.71	7	100–40,000	0.015

thickness of the momentum and thermal boundary layers. Typical Prandtl values are as listed in Table 2.8.

2.3.3.5 Schmidt Number [14, 25]

The Schmidt number is defined as the ratio of molecular momentum to mass diffusivity. It is used to characterise fluid flows in which there are simultaneous momentum and mass diffusion convection processes. It is named after Ernst Schmidt and expressed as

$$Sc = \frac{v}{D} \tag{2.68}$$

where v is the kinematic viscosity and D is the mass diffusivity.

The Schmidt number for the mass transfer is analogous to the Prandtl number for heat transfer. Its physical implication means the relative thickness of the hydrodynamic layer and mass-transfer boundary layer. The ratio of the velocity boundary layer (δ) to concentration boundary layer (δ_C) is governed by the Schmidt number. The relationship is given by

$$\frac{\delta}{\delta_C} = Sc^{1/3} \tag{2.69}$$

If the Schmidt number is 1, the two boundary layers have the same thickness. If the Schmidt number is greater than 1, the thermal boundary layer is thinner than the velocity boundary layer. If the Schmidt number is less than 1, which is the case for a CVD process operated in normal conditions, the concentration boundary layer is thicker than the velocity boundary layer.

2.4 Vapour Pressures of Chemical Vapour Deposition Precursors

For CVD processes, both liquid and solid substances are usually used as precursors. In some cases, they must be heated to the required temperature to produce sufficient supply. As shown in Figure 2.21, the vapour pressures of three liquid substances (i.e. C_2H_5OH, CCl_4 and C_6H_6Cl) are increased as the temperature increases. However, the temperature dependence of vapour pressure is not linear.
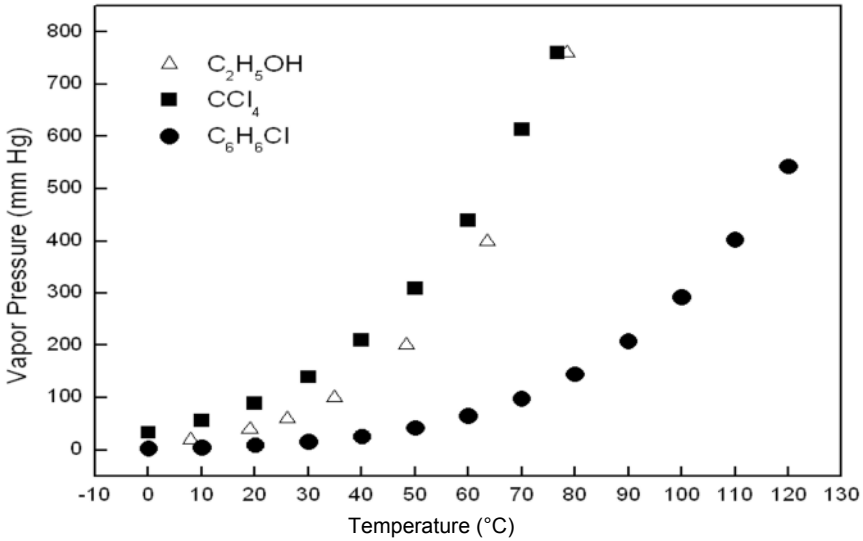
Figure 2.21. Relation of vapour pressure and temperature of liquids

The saturated vapour pressure (P) of a liquid precursor is governed by the Clausius–Clapeyron equation as follows [37, 38]:

$$\frac{dP}{dT} = \frac{\Delta H_{vap}}{T \Delta V_m} \tag{2.70}$$

where ΔH_{vap} is the enthalpy of vaporisation, ΔV_m is the change in molar volume of two phases and T is the absolute temperature in Kelvin.

It is well known that the volume of a vapour, $V_{(g)}$, is much larger than that of the equivalent amount of a liquid. As a result, it is reasonable that the $V_{(g)}$ of vapour volume represents the volume change of ΔV_m. Further, the vapour can be considered a perfect gas. Based on the state equation of perfect gases for a mole gas, the Clausius–Clapeyron equation can be rewritten as

$$\frac{d(\ln P)}{dT} = \frac{\Delta H_{vap}}{RT^2} \tag{2.71}$$

where R is the gas constant.

It is recognised that ΔH_{vap} depends only weakly on T. This equation can be integrated to give the following approximate equation:

$$\ln P = A - \frac{\Delta H_{vap}}{RT} = A - \frac{B}{T} \tag{2.72}$$

where *A* and *B* are two constants.

The Clausius–Clapeyron equation can also be applied to estimate the vapour pressure of a solid precursor. In this case, the enthalpy of sublimation (ΔH_{sub}) should replace the enthalpy of vaporisation.

Vapour pressure data of some CVD precursors are listed in Appendix B.

References

[1]   Resnick R, Halliday D, Krane KS (2002) Physics vol 1, 5th edn. Wiley, New York
[2]   Sears F W, Zemansky M W, Young H D (1987) University physics, 17th edn. Addison–Wesley, London
[3]   Roth A (1990) Vacuum technology, 3rd edn. North–Holland, New York
[4]   Knudsen M (1952) The kinetic theory of gases. Methuen, London, pp26–28
[5]   Thomas J M, Thomas W J (1997) Principles and practice of heterogeneous catalysis. VCH, Weinheim, pp85–87
[6]   Ohring M (1992) The materials science of thin films. Academic, New Jersey
[7]   Hucknall D (1991) Vacuum technology and application. Butterworth Heinemann, Oxford, UK, pp40–307
[8]   Chambers A, Fitch RK, Halliday BS (1998) Basic vacuum technology, 2nd edn. Institute of Physics, Bristol, UK
[9]   Yarwood J ed (1975) High vacuum technique, 4th revised edn. Chapman & Hall, New York, pp16–103
[10]   Harris NS (1989) Modern vacuum practice. McGraw–Hill, London, pp72–85
[11]   Levesque A, Bouteville A (2001) Evaluation of corrosion behaviour of tantalum coating obtained by low pressure chemical vapour deposition using electrochemical polarization. J Phys IV11:Pr3-915–920
[12]   Dennis NTM, Heppell TA (1968) Vacuum system design. Chapman & Hall, London
[13]   Kuhn M, Bachmann P (1987) Selection and analytical monitoring of backing pump fluids in semiconductor processes. J Vac Sci Technol A5:2534–253
[14]   Bird R B, Stewart W E, Lightfoot E N (1960) Transport phenomena. Wiley, New York
[15]   Reid RC, Prausnitz JM , Poling BE (1987) The properties of gases and liquids, 4th edn. McGraw–Hill, New York
[16]   Beek WJ, Muttzall KMK, van Heuven JW (1999) Transport phenomena, 2nd edn. Wiley, New York
[17]   Thomson WJ   (2000) Introduction to transport phenomena. Prentice Hall, Upper Saddle River, NJ
[18]   Chapman S, Cowling TG (1974) The mathematical theory of nonuniform gases, 3rd edn. Cambridge University Press, Cambridge
[19]   Hirschfelder JO, Curtiss CF, Bird RB (1954) Molecular theory of gases and liquids. Wiley, New York
[20]   Munson BR, Young DF, Okiishi TH (2006) Fundamentals of fluid mechanics, 5th edn. Wiley, New York
[21]   Vargaftik NB (1983) Handbook of physical properties of liquids and gases, pure substances and mixtures, 2nd edn. Hemisphere, Washington, DC
[22]   Wilke CR (1950) J Chem Phys 18:517
[23]   Herning F , Zipperer L (1936) Gas wasserfach 79:49
[24]   Wassiljewa A (1904) Physik Z 5:737
[25]   Ceankoplis CJ (1993) Transport processes and unit operations, 3rd edn. Prentice Hall, Engelwood Cliffs, NJ

[26]   Dullien FAL (1979) Porous media: fluid transport and pore structure. Academic, New York

[27]   Tai NH, Chou TW (1990) Modelling of an improved chemical vapor infiltration process for ceramic composites fabrication. J Am Ceram Soc 73:1489–1498

[28]   Schlichting H (1979) Boundary-layer theory, 7th edn. translated by J Kestin. McGraw–Hill, New York

[29]   Incropera FP, Dewitt DP, Bergman TL, Lavine AS (2007) Fundamentals of heat and mass transfer, 6th edn. Wiley, New York, pp348–351

[30]   Jensen KF (1993) Fundamentals of chemical vapour deposition. In: Hitchman ML, Jensen KF (eds) Chemical vapour deposition: principles and applications. Academic, New York

[31]   Choy KL (2003) Chemical vapor deposition of coatings. Prog Mater Sci 48:57–170

[32]   Jesen KF (1993) Fundamentals of chemical vapour deposition. In: Hitchman ML, Jensen KF (eds) Chemical vapour deposition: principles and applications. Academic, New York, pp31–90

[33]   Glocker DA, Shah SI (eds) (1995) Handbook of thin film process technology. Institute of Physics, Bristol, UK

[34]   Visser EP, Kleijn CR, Govers CAM., Hoogendoorn CJ, Giling LJ (1989) Return flows in horizontal MOCVD reactors studied with the use of TiO_2 particle injection and numerical calculations. J Crystal Growth 94:929–946

[35]   Ellison A, Zhang J, Peterson J, Henry A, Wahab Q, Bergman, JP, Makarov YN, Vorob'ev A, Vehanen A, Janzen E (1999) High temperature CVD growth of SiC. Mater Sci Eng B61-62:113–120

[36]   Nakamura S, Fasol G (1997) The blue laser diode. Springer, Berlin Heidelberg New York

[37]   Adam NK (1958) Physical chemistry. Oxford University Press, London

[38]   McQuarrie DA, Simon JD (1997) Physical chemistry. University Science Books, Sausalito, CA